INCORPORATION OF SVCS INTO ENERGY FUNCTION METHODS

Ian A. Hiskens, Member, IEEE

Queensland Electricity Commission
Brisbane, Australia

David J. Hill, Member, IEEE

Dept. of Electrical Engineering and Computer Science
University of Newcastle, Australia

Abstract - The incorporation of static var compensators (SVCs) into energy function methods is described in this paper. The consequences of SVCs encountering limits are of particular interest. At a limit point, the network description undergoes a change. System behaviour is not smooth. This lack of smoothness is investigated. A valid energy function, which includes the effects of SVCs and their limits, is established. Stability assessment results, obtained for a real power system, demonstrate the effects of SVC limits. It is shown that the theory developed for handling limits can be applied to models of other power system components.

Keywords - energy functions, static var compensators, reactive power limits, network model discontinuities, direct stability assessment

I INTRODUCTION

The usefulness of direct stability assessment techniques, based on energy function concepts, has been steadily improving over the last few years. Advances have been made in a number of areas. These range from speed and reliability improvements in the calculation of critical energy [1,2,3], through to improved modelling of power system components. In this latter category, advances have been made in the modelling of generators/exciters/AVRs [4,5] and of the network [6,7,8]. Realistic load modelling has been incorporated [9,10]. Therefore quite accurate modelling of traditional power systems is possible. However, the trend in many utilities, including the Queensland Electricity Commission (QEC), is to rely on static var compensators (SVCs) to enhance the power transfer capability of their transmission systems.

SVCs improve power transfer capability by regulating voltage through the (effective) variation of shunt susceptance at a bus. The resulting stabilized voltages allow a greater level of synchronizing power between machines, thus improving stability. Unlike machines, SVCs have no inertia, and so can respond extremely quickly to disturbances. However, a further difference is that SVCs offer no possibility for temporarily exceeding reactive power limits. Susceptance limits are firm, and so must be considered in direct methods.

Traditionally, energy function methods have been based on a reduced network model (RNM) of the power system. In that model, all loads are converted to constant admittance, and the network is reduced to the generator internal buses [11]. Realistic modelling of network based devices such as SVCs is therefore impossible. However, structure preserving models (SPMs) maintain the full structure (or topology) of the network [8,9]. Therefore, because of the existence of SVC buses in SPMs, they are the most appropriate system model within which to incorporate SVCs.

The contents of the paper are as follows. Section 2 firstly reviews an appropriate SPM. Modifications required to incorporate SVCs are then introduced. In Section 3, the consequences of SVCs encountering limits are considered. An energy function which takes account of SVCs, and their limits, is investigated in Section 4. In Section 5, an example illustrates the effects that SVCs have on system stability, and on stability assessment using energy function methods. Section 6 describes how the theory developed to handle the SVC limit discontinuities can be used to improve modelling of other system components.

91 SM 424-2 PWRS A paper recommended and approved by the IEEE Power System Engineering Committee of the IEEE Power Engineering Society for presentation at the IEEE/PES 1991 Summer Meeting, San Diego, California, July 28 - August 1, 1991. Manuscript submitted January 24, 1991; made available for printing June 13, 1991.

II POWER SYSTEM MODEL

In order to illustrate the modifications to the power system model which are required to include SVCs, the basic structure preserving power system model (SPM) shall initially be reviewed. More extensive details of this model are available elsewhere [8,9]. Inclusion of SVCs is then considered.

2.1 Structure Preserving Model without SVCs

The classical machine model is used in the development of this SPM. Therefore the synchronous machines are represented by a constant voltage in series with transient reactance. As mentioned earlier, other generator/exciter models could be substituted if necessary using established techniques. However those models have no bearing on the incorporation of SVCs into energy function methods, so shall not be considered further.

Consider now a network consisting of n_o buses connected by transmission lines. At m of these buses there are generators. Hence the network is augmented with m fictious buses representing the generator internal buses, in accordance with the classical machine model. The total number of buses in the augmented system is therefore $n_o+m:=n$.

Let the complex voltage at the i^{th} bus be the (time varying) phasor $V_i=|V_i|\angle\delta_i$ where δ_i is the bus phase angle with respect to a synchronously rotating reference frame. The bus frequency deviation is given by $\omega_i=\dot{\delta}_i$. The SPM of interest is based on machine reference angles, with the n^{th} bus taken as the reference. We use the internodal angles $\alpha_i:=\delta_i-\delta_n$. Define $|\underline{V}|=[|V_1|,\ldots,|V_{n_o}|]^t$, $\underline{\alpha}=[\alpha_1,\ldots,\alpha_{n-1}]^t=[\underline{\alpha}_\ell^t\ \underline{\alpha}_g^t]^t$ and $\underline{\omega}_g=[\omega_{n_o+1},\ldots,\omega_n]^t$. In [8] it is shown that the SPM can be established as

$$\dot{\underline{\omega}}_g = -\underline{M}_g^{-1}\underline{D}_g\underline{\omega}_g - \underline{M}_g^{-1}\underline{T}_g^t\underline{f}_g(\underline{\alpha}_g,\underline{\alpha}_\ell,|\underline{V}|) \quad (1a)$$

$$\dot{\underline{\alpha}}_g = \underline{T}_g\underline{\omega}_g \quad (1b)$$

$$\underline{0} = \underline{f}_\ell(\underline{\alpha}_g,\underline{\alpha}_\ell,|\underline{V}|) \quad (2a)$$

$$\underline{0} = \underline{g}(\underline{\alpha}_g,\underline{\alpha}_\ell,|\underline{V}|) \quad (2b)$$

where $\underline{M}_g, \underline{D}_g$ - diagonal matrices of inertia, damping constants

$\underline{T}_g$ - specially structured matrix of ±1 entries

$-\underline{f}_{g}$ - accel. power at generators $1,\ldots,m-1$

$\underline{f}_\ell$ - real power balance at load buses

$\underline{g}$ - reactive power balance at load buses

Note that the SPM consists of a set of differential-algebraic (DA) equations. The system variables are clearly $\underline{\omega}_g \in \mathbb{R}^m$, $\underline{\alpha}_g \in \mathbb{R}^{m-1}$, $\underline{\alpha}_\ell \in \mathbb{R}^{n_o}$ and $|\underline{V}| \in \mathbb{R}_+^{n_o}$. The system state is $(\underline{\omega}_g, \underline{\alpha}_g)$, with $(\underline{\alpha}_\ell, |\underline{V}|)$ being algebraicly dependent on that state.

The structure of the solution set for (2) is of particular importance in the analysis of this DA model. This set is defined as

$$G := \{ \underline{z} : \underline{f}_\ell(\underline{z})=\underline{0} \ , \ \underline{g}(\underline{z})=\underline{0} \} \qquad (3)$$

where $\underline{z} = (\underline{\alpha}_g, \underline{\alpha}_\ell, |\underline{V}|)$. Typically G is a differentiable (m-1)-manifold. This manifold shall be referred to as the *constraint manifold*.

2.2 SVC Modelling

A model of an SVC control system, suitable for transient stability studies, is shown in Figure 1. It is typical of models used by industry for this type of study [12]. Descriptions of the components of this model follow. Details of modifications needed to the SPM to include these various aspects of SVCs are explained.

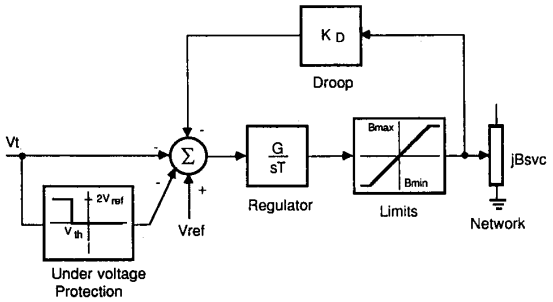

Figure 1: SVC Control System

2.2.1 Regulator

In general, integral control is used to regulate the output of SVCs [13]. This is indicated in Figure 1. Any error between the sensed voltage V_t and the reference voltage V_{ref} is integrated, resulting in an adjustment to the thyristor firing angle. This alters the effective susceptance at the SVC bus. SVC control system design is based on the assumption that increased capacitance at a bus will cause its voltage to rise. This is generally the case, but may not necessarily be true. Conditions affecting the validity of this assumption are considered further in [14]. Under normal operating conditions however, power systems do behave in the appropriate way. Therefore, in the following analysis, we shall assume:

A1. Increasing capacitance at a bus causes its voltage to rise.

SVCs can respond to voltage changes extremely quickly because their regulator time constants T are generally small. Step response tests performed on an SVC in the QEC system have confirmed this [15]. In fact, compared with the response of generators, SVCs can be thought of as responding instantaneously [16]. This extremely fast behaviour enables a simplification of the SVC model in accordance with the following assumption:

A2. SVCs respond instantaneously to voltage fluctuations.

Assumption A2 ensures that the regulated bus voltage remains constant, so it can be treated as a PV-type bus. Real power and voltage magnitude are specified, while reactive power and voltage angle are unknown. A modification to the algebraic equations of the SPM (2) must be made to incorporate PV buses. Let the number of SVC buses be n_s , and label them $i=n_o-n_s+1,\ldots,n_o$, i.e., the last n_s load buses. Partition $\underline{g}$, $|\underline{V}|$ as $\underline{g}^t = [\ \underline{g}_\ell^t \ \ \underline{g}_s^t\ ]$ and $|\underline{V}|^t = [\ |\underline{V}_\ell|^t \ \ |\underline{V}_s|^t\ ]$, where $\underline{g}_\ell$, $|\underline{V}_\ell|$ are n_o-n_s vectors referring to load buses, and $\underline{g}_s$, $|\underline{V}_s|$ are n_s vectors referring to SVC buses. Note that the voltages at SVC buses are constant, i.e., $|\underline{V}_s| = |\underline{V}_s^o|$ for some constant $|\underline{V}_s^o|$. Also note that reactive power is not constrained at SVC buses, so functions $\underline{g}_s$ are not constraints of the model. Accordingly, the SPM becomes

$$\dot{\underline{\omega}}_g = -\underline{M}_g^{-1}\underline{D}_g\underline{\omega}_g - \underline{M}_g^{-1}\underline{T}_g^t\underline{f}_g(\underline{\alpha}_g, \underline{\alpha}_\ell, |\underline{V}_\ell|) \qquad (4a)$$

$$\dot{\underline{\alpha}}_g = \underline{T}_g\underline{\omega}_g \qquad (4b)$$

$$\underline{0} = \underline{f}_\ell(\underline{\alpha}_g, \underline{\alpha}_\ell, |\underline{V}_\ell|) \qquad (5a)$$

$$\underline{0} = \underline{g}_\ell(\underline{\alpha}_g, \underline{\alpha}_\ell, |\underline{V}_\ell|) \qquad (5b)$$

The system state is still $(\underline{\omega}_g, \underline{\alpha}_g)$, but the algebraic variables are now $(\underline{\alpha}_\ell, |\underline{V}_\ell|) \in \mathbb{R}^{2n_o-n_s}$. The number of algebraic equations has also been reduced to $2n_o-n_s$. Once again the constraint manifold is defined as the solution set of the algebraic equations (5).

2.2.2 Limits

SVC susceptance is composed of fixed capacitors and thyristor controlled reactors (TCRs). Therefore unlike generators, where reactive power limits can be temporarily exceeded, susceptance limits of an SVC are firm. Maximum capacitance is achieved when the TCR is fully blocked, i.e., no current is allowed to pass, while maximum inductance occurs when the TCR is fully pulsed, i.e., no chopping of the TCR current. In this latter case the net susceptance is achieved from a parallel connection of the fixed capacitors and the TCRs.

Because the susceptance limits are fixed, they must be modelled. Ignoring them would be equivalent to assuming SVCs had unlimited capacity to support voltage during transients. Optimistic (and unreliable) stability results would be obtained. When a limit is encountered, voltage can no longer be controlled, so the bus ceases to behave as a PV bus. The limit also introduces a reactive power constraint. Therefore the bus type changes from PV to PQ. The number of SVCs is effectively reduced by one. The SVC bus becomes like any other load bus with non-zero susceptance. The number of algebraic variables increases by one, $|V_i|$, and the number of algebraic constraints also increases by one, g_i . Of course, when the SVC comes off the limit, the voltage again becomes constrained, and the

reactive power unconstrained.

If the SVC encounters, or comes off, a limit as the power system swings in response to a disturbance, a discontinuity occurs in the rate of change of $\underline{f}_g$. This follows from a comparison of the SPMs with and without SVCs. A detailed investigation of the effects of limits is undertaken in Section 3.

Example 1

The two generator power system of Figure 2 can be used to illustrate SVC limit behaviour. The responses to a 50MW load increase at GEN2 are shown in Figure 3. Note that at the point where the SVC encounters a limit, f_{GEN2} is continuous but has a step change in time derivative. □

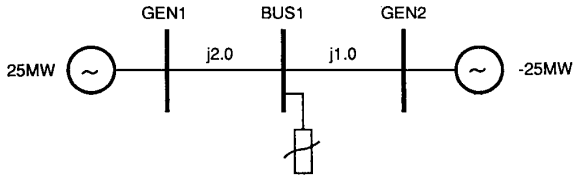

Figure 2: Two Generator System With SVC

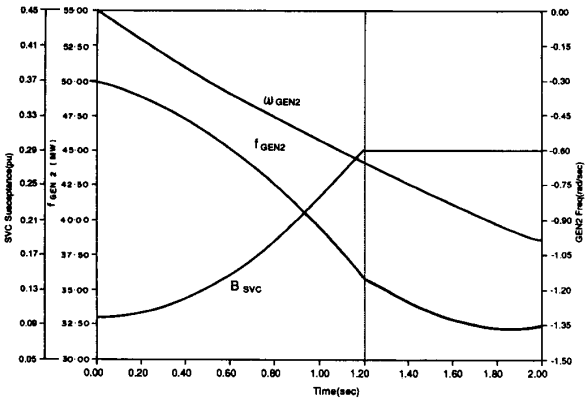

Figure 3: Transient Response to a Load Step

2.2.3 Undervoltage Operation

In response to a power system fault, local SVCs, if allowed to operate normally, would sense low voltage and respond by driving susceptances to their capacitive limits. Upon fault clearing, bus voltages would peak at unacceptable levels. To overcome this undesirable behaviour, most SVCs are equipped with undervoltage detection equipment [13]. Should the voltage fall below a preset threshold, a large negative offset is applied to the summing junction. This causes SVC susceptance to very quickly reach its inductive limit, where it remains until the fault is removed.

During the faulted period the SVC therefore behaves as a fixed susceptance, at its inductive limit. The SVC bus can be accurately modelled as a PQ bus. Note though that undervoltage action is only of importance in determining the system state at fault clearing. It plays no part in the post-fault dynamics.

2.2.4 Droop Characteristic

To reduce SVC susceptance excursions, the regulating behaviour of SVCs is often modified so that it follows a *droop* characteristic [13]. Droop has the effect of varying the SVC regulated voltage depending upon the value of SVC susceptance. As susceptance goes more capacitive, the regulated voltage reduces, and vice versa. Figure 1 shows that droop is implemented in the control system as a feedback loop through the droop constant K_D.

The implementation of this control system feature into a network based model can be achieved by recognizing that feedback droop has exactly the same effect as if the SVC was regulating (to a constant voltage) a fictious internal bus behind an appropriate reactance. This equivalent network arrangement is shown in Figure 4. It is established in [17] that the reactance X_D is related to the droop constant by $X_D = \frac{K_D}{V_o}$, where V_o is the SVC reference voltage.

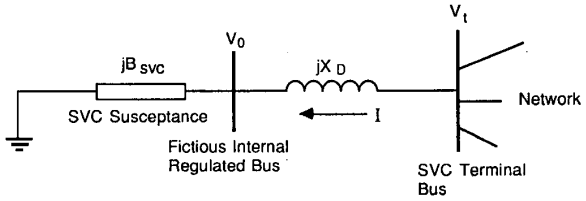

Figure 4: SVC Droop Equivalent Network

Droop is implemented into the SPM via this equivalent network. An extra 'internal' SVC bus is introduced, as in Figure 4. It is modelled as a PV bus. The SVC terminal bus is then modelled as a PQ bus.

2.3 Local ODE Representation of the SPM

It is shown in [9] that the DA system describing the SPM (either with or without SVCs) is locally equivalent to a set of ordinary differential equations for almost all operating states. This result follows from the implicit function theorem [18]. Consider the SPM without SVCs (1),(2), and define the Jacobian

$$\underline{J}_{\ell\ell} = \begin{bmatrix} \frac{\partial \underline{f}_\ell}{\partial \underline{\alpha}_\ell} & \frac{\partial \underline{f}_\ell}{\partial |\underline{V}|} \\ \frac{\partial \underline{g}}{\partial \underline{\alpha}_\ell} & \frac{\partial \underline{g}}{\partial |\underline{V}|} \end{bmatrix} \in \mathbb{R}^{2n_o \times 2n_o} \qquad (6)$$

If $\det \underline{J}_{\ell\ell} \neq 0$, locally the load bus variables can be written explicitly in terms of the generator angles as

$$\underline{\alpha}_\ell = \underline{\phi}(\underline{\alpha}_g) \quad , \quad |\underline{V}| = \underline{\psi}(\underline{\alpha}_g) \qquad (7)$$

An equivalent differential equation form of the SPM can therefore be obtained locally by substituting (7) into (1a). Setting

$$\underline{f}_g^*(\underline{\alpha}_g) := \underline{f}_g(\underline{\alpha}_g, \underline{\phi}(\underline{\alpha}_g), \underline{\psi}(\underline{\alpha}_g)) \qquad (8)$$

gives the model

$$\dot{\underline{\omega}}_g = -\underline{M}_g^{-1}\underline{D}_g\underline{\omega}_g - \underline{M}_g^{-1}\underline{T}_g^t\underline{f}_g^*(\underline{\alpha}_g) \qquad (9a)$$

$$\dot{\underline{\alpha}}_g = \underline{T}_g\underline{\omega}_g \qquad (9b)$$

Equations (9) define ordinary differential equations which are locally equivalent to the SPM. In [19], this local solvability is extended to solvability over disjoint regions, called causal regions. All following analysis shall be based on the assumption:

A3. The system remains within a single causal region.

Assumption A3 is justified because SVCs do not introduce any new factors into the discussion of boundary behaviour. That behaviour is investigated in [17].

The local form (9) shall prove useful in analysing system behaviour when limits are encountered.

III EFFECTS OF SVC LIMITS ON CONSTRAINT MANIFOLD

As a power system moves in response to a disturbance, it is likely that SVCs will encounter limits, usually capacitive limits. This occurs generally because increased reactive power is required to support sagging voltages. These result from higher flows across the network, between swinging groups of generators.

The essential ideas behind the analysis of limiting behaviour of SVCs are not dependent on the number of SVCs in the system. Therefore, to maintain clarity in the following development, it shall be assumed that the network contains a single SVC, at bus j. We initially investigate the distortion of the constraint manifold caused by limits. The effects of this distortion on $\underline{\Phi}$ and $\underline{\Psi}$ of (7), and hence $\underline{f}_g^*(\underline{\alpha}_g)$ of (8) are then established.

Consider a power system with an asymptotically stable EP at which the SVC is regulating. That EP must be surrounded by a region of the constraint manifold where the SVC does not encounter a limit. Define the *regulating region* as

$$\mathfrak{R}_j = \{ \underline{z} : \underline{f}_\ell(\underline{z})=\underline{0} \ , \ \underline{g}_\ell(\underline{z})=\underline{0} \ , \ |V_j|=|V_j^\circ| \ , \ B_{lo,j} < \frac{1}{|V_j|^2} Q_{bj}(\underline{z}) < B_{hi,j} \}$$

where Q_{bj} is the reactive power leaving bus j via transmission lines, $B_{lo,j}$ and $B_{hi,j}$ are the inductive and capacitive susceptance limits respectively and $|V_j^\circ|$ is the setpoint voltage. This region is in general at least partially bounded by points at which the SVC encounters a limit. At such a limit point, SVC susceptance reaches its maximum inductive or capacitive value.

At a point where a limit is encountered, SVC bus voltage remains at its setpoint value. (It only starts to deviate after this point.) However the additional reactive power balance constraint

$$g_j(\underline{\alpha}_g, \underline{\alpha}_\ell, |\underline{V}|) = |V_j|^{-1}(Q_{bj}(\underline{\alpha}_g, \underline{\alpha}_\ell, |\underline{V}|) - B_{lim,j}|V_j|^2) = 0 \qquad (10)$$

must be satisfied. Note that $B_{lim,j}$ is the SVC susceptance at the appropriate limit. Define the set of points at which a limit is encountered as the *limit surface*,

$$\mathfrak{S}_j = \{ \underline{z} : \underline{f}_\ell(\underline{z})=\underline{0} \ , \ \underline{g}_\ell(\underline{z})=\underline{0} \ , \ g_j(\underline{z})=0 \ , \ |V_j|=|V_j^\circ| \}$$

Points in $\mathfrak{S}_j$ satisfy all the constraints of $\mathfrak{R}_j$, plus the reactive power constraint (10).

Once a limit has been encountered, SVC bus voltage can no longer be regulated, so the network description must change. The constraint governing SVC bus voltage is replaced by the reactive power constraint (10). It is then possible to define the region where the SVC is operating on a limit as

$$T_j = \{ \underline{z} : \underline{f}_\ell(\underline{z})=\underline{0} \ , \ \underline{g}_\ell(\underline{z})=\underline{0} \ , \ g_j(\underline{z})=0 \ , \ |V_j|>|V_j^\circ| \text{ if } B_{lim,j}=B_{lo,j} \ , \ |V_j|<|V_j^\circ| \text{ if } B_{lim,j}=B_{hi,j} \}$$

This shall be referred to as the *limit region*. Points in $\mathfrak{S}_j$ satisfy all the constraints of T_j, plus the setpoint voltage constraint $|V_j|=|V_j^\circ|$. Note that the voltage inequalities of this definition rely on assumption A1.

It is shown in [17] that in general $\mathfrak{R}_j$ and T_j define differentiable (m-1)-manifolds, (with boundaries). $\mathfrak{S}_j$ defines a differentiable (m-2)-manifold. Network solutions are fully described by the *constraint surface*

$$G' = \mathfrak{R}_j \cup \mathfrak{S}_j \cup T_j$$

The structure of $\mathfrak{R}_j$, $\mathfrak{S}_j$ and T_j ensure that G' is a continuous surface [17]. Note however that G' is not smooth at points in $\mathfrak{S}_j$.

G' takes the place of the constraint manifold G in situations where SVC limits are important. However, because G' is not differentiable, the terminology constraint surface is more appropriate than constraint manifold.

Because the constraint surface is not smooth, the implicit function theorem is not directly applicable. Therefore the functions $\underline{\Phi}$, $\underline{\Psi}$ cannot immediately be defined. However, away from the limit surface, the regulating region and the limit region are smooth, so the required functions $\underline{\Phi}_r$, $\underline{\Psi}_r$ and $\underline{\Phi}_t$, $\underline{\Psi}_t$ are locally defined. These regions are open, but they approach the limit surface arbitrarily closely. Therefore, using the fact that the constraint surface is continuous at the limit surface, it is shown in [17] that the function $\underline{\Phi}$, composed of $\underline{\Phi}_r$ and $\underline{\Phi}_t$ joining at the limit surface, is continuous. Likewise $\underline{\Psi}$, composed of $\underline{\Psi}_r$ and $\underline{\Psi}_t$, is also continuous. Neither of these functions is differentiable at the limit surface however. Therefore $\underline{\Phi}$, $\underline{\Psi} \in C^\circ$.

Within a causal region, the generator powers are given locally by (8). Because $\underline{\Phi}$, $\underline{\Psi}$ are continuous, $\underline{f}_g^*(\underline{\alpha}_g)$ will be continuous. However the Jacobian of $\underline{f}_g^*(\underline{\alpha}_g)$ will undergo a step change at the limit surface. (This Jacobian is dependent on $J_{\ell\ell}$. The structure of $J_{\ell\ell}$ changes at the limit surface, as its dimension is altered by 1 due to the addition/deletion of a constraint and variable.) Therefore $\underline{f}_g^* \in C^\circ$.

Example 2

The simple two generator network of Figure 2 can be used to illustrate the effect of SVC limits. Figure 5 shows P-α_g curves (effectively $\underline{f}_g^*(\underline{\alpha}_g)$) for this system, for various values of limits. For comparison purposes, the case where the limits are zero, i.e., no SVC, is also included. As predicted, for non-zero limits, these curves are continuous, but have discontinuous derivatives. Note that higher limits allow greater power flow across the network. □

IV ENERGY FUNCTIONS

In this section, we establish an energy function which incorporates SVCs, including limiting effects. As background, we initially review an energy function which is commonly used for the basic SPM.

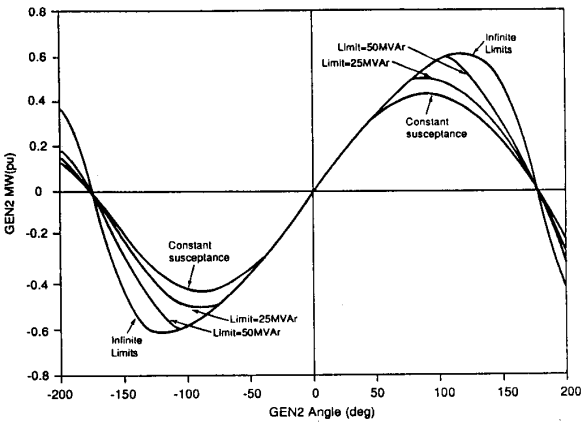

Figure 5: P-α_g Curves for Various SVC Limits

4.1 Energy Function for the SPM

The development of an energy function for the SPM has been studied previously using first integral and Luré problem analysis methods [7,20,21,8]. A useful energy function is given by

$$V(\underline{\omega}_g,\underline{z}) = \tfrac{1}{2}\,\underline{\omega}_g^t \underline{P}_1(\mu)\underline{\omega}_g + \int_{\underline{z}^s}^{\underline{z}} \langle \underline{h}(\underline{\lambda}), d\underline{\lambda}\rangle \qquad (11)$$

where $\underline{z} = (\underline{\alpha}_g, \underline{\alpha}_\ell, |\underline{V}|)$, $\underline{h}(\underline{z}) = \left[\underline{f}_g(\underline{z}), \underline{f}_\ell(\underline{z}), \underline{g}(\underline{z})\right]$ and $\underline{z}^s$ denotes a stable EP. Note that $\underline{P}_1(\mu)$ must satisfy $\underline{P}_1(\mu)>0$. Conditions governing this matrix are discussed in [8]. The first term of (11) is often referred to as the kinetic energy function, whilst the other term is known as the potential energy function.

4.2 Energy Function with SVCs

Referring to (11), the kinetic energy term of the energy function is independent of the algebraic functions, so no modification to that term is necessary to account for SVCs. However the potential energy term becomes

$$PE_{svc}(\tilde{\underline{z}}) = \int_{\tilde{\underline{z}}^s}^{\tilde{\underline{z}}} \langle \tilde{\underline{h}}(\underline{\lambda}), d\underline{\lambda}\rangle \qquad (12)$$

where $\tilde{\underline{z}} = (\underline{\alpha}_g, \underline{\alpha}_\ell, |\underline{V}_\ell|)$, $\tilde{\underline{h}}(\tilde{\underline{z}}) = \left[\underline{f}_g(\tilde{\underline{z}}), \underline{f}_\ell(\tilde{\underline{z}}), \underline{g}_\ell(\tilde{\underline{z}})\right]$. This potential energy function can be evaluated as

$$PE_{svc}(\tilde{\underline{z}}) = - \tfrac{1}{2}\sum_{i=1}^{n}\sum_{j=1}^{n} B_{ij}\left[|V_i||V_j|\cos\alpha_{ij} - |V_i^s||V_j^s|\cos\alpha_{ij}^s\right] - \int_{\underline{\alpha}^s}^{\underline{\alpha}} \underline{P}(|\underline{V}|)^t d\underline{\alpha} + \sum_{i=1}^{n_o-n_s}\int_{|V_i^s|}^{|V_i|} \frac{Q_{di}(\tau_i)}{\tau_i}\, d\tau_i \qquad (13)$$

where $\underline{P}(|\underline{V}|)$ is the vector of real power injections at each bus, and $Q_{di}(|V_i|)$ is the reactive power demand at bus i . The only difference between (13) and the evaluation of the potential energy term of (11) lies in the last summation term. The fact that $V_{svc} = KE + PE_{svc}$ is an energy function follows directly from (11) being an energy function.

Note

If real power loads were constant, i.e., did not vary with voltage, then (13) would satisfy all the conditions of a Lyapunov function. In reality however, loads vary with voltage, so the integral $\int_{\underline{\alpha}^s}^{\underline{\alpha}} \underline{P}(|\underline{V}|)^t d\underline{\alpha}$ is path dependent. The details of approximating this type of integral are well documented [11,17].

4.3 Effects of Limits

It can be seen from (11),(12) that the potential energy function is dependent on the algebraic variables $\underline{\alpha}_\ell$, $|\underline{V}|$. But in Section 2.3, it was indicated that within each causal region, there exist unique continuous functions $\underline{\alpha}_\ell = \underline{\Phi}(\underline{\alpha}_g)$ and $|\underline{V}| = \underline{\Psi}(\underline{\alpha}_g)$. This result was extended in Section 3 to show that even when limits are encountered, $\underline{\Phi}$ and $\underline{\Psi}$ still exist. Therefore, referring to (8), the potential energy function on any causal region may be written,

$$PE^*(\underline{\alpha}_g) = \int_{\underline{\alpha}_g^s}^{\underline{\alpha}_g} \langle \underline{f}_g(\underline{\alpha}_g, \underline{\Phi}(\underline{\alpha}_g), \underline{\Psi}(\underline{\alpha}_g)), d\underline{\alpha}_g\rangle = \int_{\underline{\alpha}_g^s}^{\underline{\alpha}_g} \langle \underline{f}_g^*(\underline{\alpha}_g), d\underline{\alpha}_g\rangle \qquad (14)$$

These local potential energy functions are dependent on $\underline{\alpha}_g$ only, so may be conceptualized as (m-1)-hypersurfaces (or *sheets*) in $\underline{\alpha}_g$-space. Note that each $PE^*(\underline{\alpha}_g)$ is unique over its causal region. Further information on these potential energy sheets may be found in [9,17,19].

It was shown in Section 3 that if SVCs encounter limits, then $\underline{f}_g^*$ is C^0 . Therefore $PE^*(\underline{\alpha}_g)$ must be C^1 , i.e., continuous with a continuous derivative. Hence, if $PE^*(\underline{\alpha}_g)$ was an increasing (decreasing) function before a limit was encountered, it must continue to increase (decrease), at least in the short term, after the limit has been enforced. Further, it is shown in [17] that the sign of $\dot{V}$ is not affected by the network change at the limit surface. Hence V remains an energy function even when SVC limits are encountered.

Example 3

Again the simple two generator network of Figure 2 can be used to illustrate SVC limit effects. Figure 6 shows the potential energy curves which correspond to the limit cases of Figure 5. These curves are smooth (in fact C^1) functions. Notice that as SVC limits are increased, the height of the potential energy well, and hence the stability margin, also increases. □

4.4 SVC Contribution to Potential Energy

It is easily shown that the double summation term of the potential energy function (13) may be evaluated as

$$- \tfrac{1}{2}\sum_{i=1}^{n}\sum_{j=1}^{n} B_{ij}\left[|V_i||V_j|\cos\alpha_{ij} - |V_i^s||V_j^s|\cos\alpha_{ij}^s\right] = \tfrac{1}{2}\sum_{i=1}^{n}\left[Q_{bi}(\underline{\alpha}, |\underline{V}|) - Q_{bi}(\underline{\alpha}^s, |\underline{V}^s|)\right] \qquad (15)$$

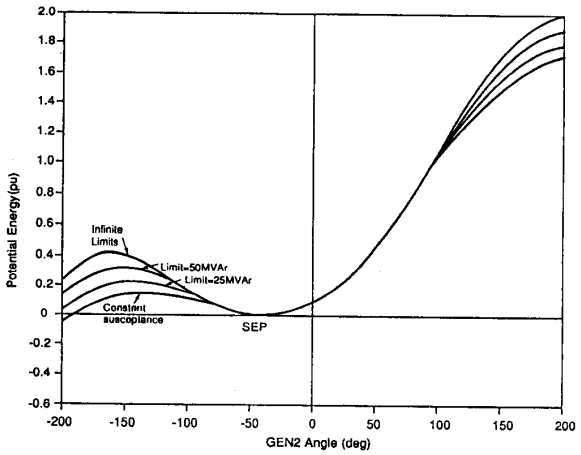

Figure 6: Potential Energy Curves for Various SVC limits

where Q_{bi} is the reactive power leaving bus i . The reactive power leaving an SVC bus is equal to the SVC susceptance times the bus voltage squared. Therefore, when not on a limit, each SVC's contribution to (15) is given by,

$$\tfrac{1}{2}\left[B_{svc,i}|V_i^o|^2 - B^s_{svc,i}|V_i^o|^2\right] = \tfrac{1}{2}|V_i^o|^2(B_{svc,i} - B^s_{svc,i}) \quad (16)$$

where $B_{svc,i}$ is the present value of SVC susceptance, $B^s_{svc,i}$ is the value at the stable EP, and $|V_i^o|$ is the setpoint voltage. Referring to (13), the SVC bus in this case does not contribute to the other (last) reactive power summation term of the potential energy function. Therefore the total contribution to potential energy of each regulating SVC is given by (16).

However, when the SVC is on a limit, its contribution to (15) becomes

$$\tfrac{1}{2}\left[B_{lim,i}|V_i|^2 - B^s_{svc,i}|V_i^o|^2 \right] \quad (17)$$

Further, because in this case SVC susceptance is constrained at its limit value, it acts as the load

$$Q_{di} = - B_{lim,i}\,|V_i|^2 \quad (18)$$

i.e., the reactive power absorbed by the (fixed) SVC susceptance. It therefore contributes to the last summation term of (13). This contribution is

$$\int_{|V_i^o|}^{|V_i|} -B_{lim,i}\,\tau_i\,d\tau_i = \tfrac{1}{2}\left[-B_{lim,i}|V_i|^2 + B_{lim,i}|V_i^o|^2\right] \quad (19)$$

The total contribution of each limited SVC to the system potential energy is the sum of (17) and (19), i.e.,

$$\tfrac{1}{2}\left[B_{lim,i}|V_i^o|^2 - B^s_{svc,i}|V_i^o|^2\right] = \tfrac{1}{2}|V_i^o|^2(B_{lim,i} - B^s_{svc,i})$$

Notice the similarity between this term and (16). Therefore, whether an SVC is on a limit or not, its contribution to potential energy depends solely on the setpoint voltage, the initial value of susceptance, and the current value of susceptance. The actual bus voltage is not important.

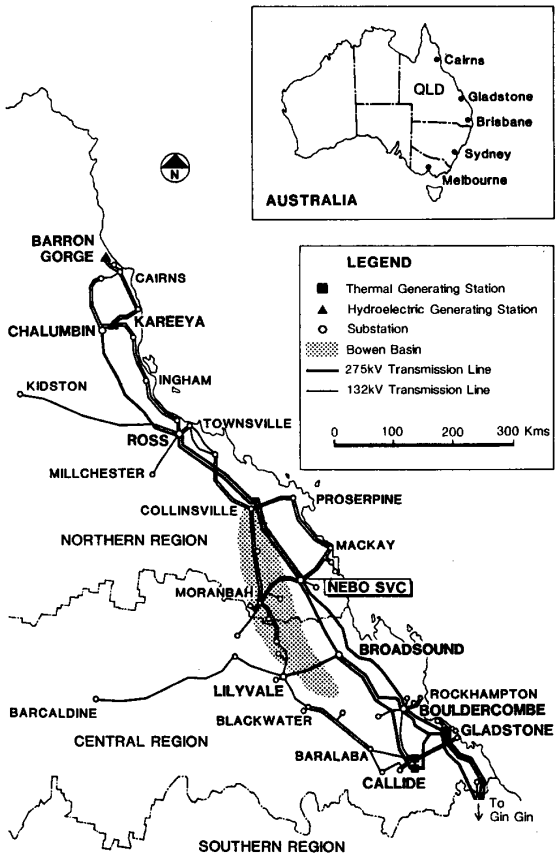

Figure 7: Northern QEC Power System

V EXAMPLE

The northern section of the Queensland Electricity Commission power system, shown in Figure 7, contains an SVC which has a significant influence on dynamic behaviour of that system. It is therefore an appropriate system to use to examine the sensitivity of direct stability assessment to SVC limits. Complete data for this system can be found in [17].

The direct stability assessment algorithm used to produce the results of this section was based on the "controlling UEP" method of determining critical energy [22,17]. This method follows from observations that as a power system approaches instability, a coherent group of generators will tend to separate from the rest of the system. This grouping of generators is referred to as the *mode of instability*. A different UEP corresponds to each mode of instability. Each fault causes generators to group according to a particular mode, and hence can be associated with a controlling UEP. The critical energy for a fault is evaluated as the potential energy at that controlling UEP. For the cases considered in this section, the generators at Kareeya and Barron Gorge separated as a group from the other generators of the system. Therefore in each case the predicted critical energy was calculated as the potential energy at the UEP corresponding to that mode of instability.

To investigate the effect of SVC limits on direct stability assessment, a three phase fault at Broadsound was simulated. This fault was cleared by the tripping

of the 275kV feeder between Broadsound and Nebo. Load indices of 1.0 and 3.0 were used for all real and reactive power loads respectively. A number of different values of the capacitive susceptance limit at Nebo SVC were tried. Results are given in Table 1. Note that the actual capacitive susceptance limit of Nebo SVC is 2.60pu. It is not surprising that as the limit increased, so did the critical clearing time and the critical energy. This is consistent with the results of Example 3.

SVC Max Limit (pu)	Predicted		Simulated	
	Critical Clearing Time	Crit Energy	Critical Clearing Time	Crit Energy
2.10	0.124	0.464	0.116 - 0.118	0.422
2.60	0.148 - 0.150	0.656	0.142 - 0.144	0.601
2.85	0.162 - 0.164	0.786	0.152 - 0.154	0.690

Table 1: SVC Limit Sensitivity.

For each value of SVC limit, good agreement was obtained between the critical values predicted by the stability assessment algorithm and the actual values determined by simulation. When the limit was 2.10pu, the error in critical clearing time was 6.0% or 7ms. For the limit at 2.60pu, the error was 4.2%(6ms). A limit of 2.85pu resulted in a 6.5%(10ms) error.

It is generally expected that energy function methods give conservative predictions of system stability, i.e., predicted critical clearing time is less than the actual critical value. However the results of Table 1 are not of that form. The following arguments should help to clarify this unexpected trend.

If all real power loads in the system were modelled as constant power, then the energy function V_{svc} would be a Lyapunov function [8,17]. Because Lyapunov stability theory provides sufficient, but not necessary, conditions for stability, results in this case would always be conservative [11]. Simulations of the system of Figure 7, with constant power loads, were initiated at many locations in generator angle space, with a number of different initial generator velocity vectors. Results were in complete agreement with the theory, i.e., all cases where the initial energy was less than the critical energy were stable. (In those cases which were predicted to be unstable, but which were actually stable, the largest error in predicted ctitical energy was 3%.) One of the stable cases is shown in Figure 8. Notice in this figure that the SVC periodically encounters its capacitive susceptance limit of 2.60pu. At those points, the SVC bus voltage falls. Potential energy varies smoothly through those points, and total system energy remains constant. The unexpected results of Table 1 are therefore not related to the energy function modifications which result from the incorporation of SVCs.

However, as mentioned in Section 4.2, voltage dependent loads introduce path dependent terms into the potential energy function (13). These terms must be approximated, making results (potentially) system and disturbance dependent. It would appear that the results of Table 1 suffer slightly from this approximation.

It is not possible, using currently available approximations for the path dependent terms, to predict whether a direct stability assessment algorithm will give conservative or optimistic results. However

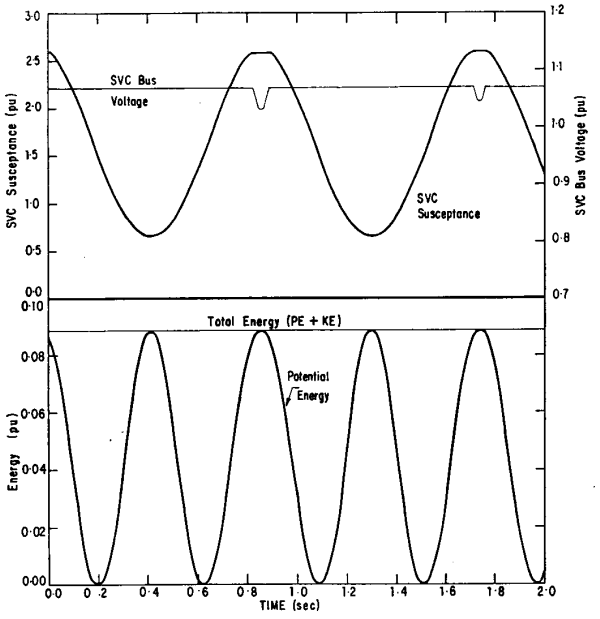

Figure 8: SVC and Energy Response at a Limit

provided that the absolute errors are small, as they are in Table 1, direct stability assessment is still extremely useful. In the stability assessment application being developed for the QEC, the energy acquired by the power system during a disturbance is compared with the predicted value. If the system energy is greater than a predefined percentage (perhaps 85%) of the critical value, the case is flagged for more detailed investigation. Such a comparison ensures that all instability situations are identified, whilst filtering off cases of little interest.

VI OTHER C^0 CONSTRAINT SURFACES

The theory developed in Sections 3 and 4 for continuous, but non-smooth, constraints, need not be restricted to SVC limiting. Other power system components may be described by similar types of constraints. In fact, by removing the smoothness restrictions, more accurate models may be possible. As with SVC limits, the only consequence of non-smooth constraints is a C^0 constraint surface, with the corresponding energy function being C^1 .

The most obvious extension of the theory is to generator reactive power limits. These limits must be considered in the application of energy function methods to the voltage stability problem [23]. By slightly adapting the results of Sections 3 and 4, the energy function term that was proposed in [23] for handling generator limits can be theoretically justified.

As a further example, the accuracy of load modelling could be improved through the use of C^0 constraints. It is recognized that often load models of the form $P_{di}=P^o_{di}|V_i|^{\zeta_i}$ are not accurate over a large range of voltages. The voltage indices themselves are voltage dependent. An improvement would result from the use of different indices over different voltage ranges. Consider the real power demand at bus i . The voltage dependence of this load may be described by

$$\left.\begin{aligned} P_{di}(|V_i|) &= P^1_{di}|V_i|^{\zeta_{1i}} && |V_i| \geq |V^1_i| \\ &= P^2_{di}|V_i|^{\zeta_{2i}} && |V^1_i| > |V_i| \geq |V^2_i| \\ &\vdots && \vdots \\ &= P^k_{di}|V_i|^{\zeta_{ki}} && |V^{k-1}_i| > |V_i| \end{aligned}\right\} \quad (20)$$

where

$$P^1_{di}|V^1_i|^{\zeta_{1i}} = P^2_{di}|V^1_i|^{\zeta_{2i}}$$
$$\vdots$$
$$P^{k-1}_{di}|V^{k-1}_i|^{\zeta_{k-1,i}} = P^k_{di}|V^{k-1}_i|^{\zeta_{ki}}$$

The constraint $f_i(\underline{\alpha}_g, \underline{\alpha}_\ell, |\underline{V}|) = 0$ is continuous because at each point where the load index changes, the power demand is uniquely defined. However, a step change occurs in the Jacobian at those points. This is similar to SVC limits, and can be analysed in exactly the same way. Again the constraint surface is C^0, and the energy function C^1. Further, as in the case of SVC limits, the energy function is locally positive definite, with a negative semi-definite derivative along trajectories.

Hence, rapid stability assessment is possible using load models of the form given by (20).

VII CONCLUSIONS

This paper describes the incorporation of static var compensators (SVCs) into an energy function method. This innovation is based on the fact that SVCs respond to disturbances much more quickly than do machines. Therefore, using a structure preserving model (SPM) of the power system, SVCs can be accurately represented as constant voltage (PV) buses.

Any accurate SVC model must take account of susceptance limits. When a limit is encountered, voltage regulation ceases. A change occurs in the network description. The paper shows that at a limit point, system response is continuous, but not smooth.

Only a minor modification is required to the usual SPM energy function to include SVCs. It is shown that even when SVCs encounter limits, the energy function is smooth, though this smoothness is restricted to C^1, i.e., the energy function is continuous with a continuous derivative. The paper indicates that the theory developed to investigate the effects of SVC limits can also be applied to models of other power system components.

The paper highlights the difficulties associated with the approximation of the path dependent integral terms introduced into the potential energy function by voltage dependent real power loads. It is concluded that this issue warrants further investigation.

VIII REFERENCES

1. P. Varaiya, F.F. Wu and R-L. Chen, "Direct Methods for Transient Stability Analysis of Power Systems: Recent Results", *Proc. IEEE*, Vol. 73, No. 12, pp 1703-1715, December 1985.
2. A.A. Fouad et. al., "Direct Transient Stability Analysis Using Energy Functions: Application to Large Power Networks", *IEEE Trans. on Power Systems*, Vol. PWRS-2, No. 1, February 1987.
3. H.D. Chiang, F.F. Wu and P.P Varaiya, "Foundations of the Potential Energy Boundary Surface Method for Power System Transient Stability Analysis", *IEEE Trans. on Circuits and Systems*, Vol. CAS-35, No. 6, pp 160-172, June 1988.
4. M.A. Pai, *Energy Function Analysis for Power System Stability*, Kluwer Academic Publishers, Boston/Dordrecht/London, 1989.
5. A.A. Fouad et. al., "Direct Transient Stability Assessment with Excitation Control", *IEEE Trans. on Power Systems*, Vol. PWRS-4, No. 1, February 1989.
6. A.R. Bergen and D.J. Hill, "A Structure Preserving Model for Power System Stability Analysis", *IEEE Trans. on Power Apparatus and Systems*, Vol. PAS-100, No. 1, pp 25-35, January 1981.
7. N. Narasimhamurthi and M.T. Musavi, "A General Energy Function for Transient Stability Analysis of Power Systems", *IEEE Trans. on Circuits and Systems*, Vol. CAS-31, No. 7, pp 637-645, July 1984.
8. D.J. Hill and C.N. Chong, "Lyapunov Functions of Luré-Postnikov Form for Structure Preserving Models of Power Systems", *Automatica*, Vol. 25, No. 3, pp 453-460, 1989.
9. I.A. Hiskens and D.J. Hill, "Energy Functions, Transient Stability and Voltage Behaviour in Power Systems with Nonlinear Loads", *IEEE Trans. on Power Systems*, Vol. PWRS-4, No. 4, pp 1525-1533, November 1989.
10. V. Vittal et. al., "Incorporation of Nonlinear Load Models in the Transient Energy Function Method", *IEEE Trans. on Power Systems*, Vol. PWRS-4, No. 3, pp 1031-1036, August 1989.
11. M.A. Pai, *Power System Stability*, North-Holland Pub. Co., New York, 1981.
12. ASEA Transmission, *SIMPOW Power System Simulator User's Manual*, Vol. 2, Vasteras, Sweden, November 1987.
13. S. Torseng, "Shunt-connected Reactors and Capacitors Controlled by Thyristors", *IEE Proc., Part C*, Vol. 128, No. 6, pp 366-373, November 1981.
14. I.A. Hiskens and C.B. McLean, "SVC Behaviour Under Voltage Collapse Conditions", presented at IEEE PES 1991 Summer Meeting, San Diego, July 1991.
15. A.J. Jenner and C.J. Oxenham, "Planning and Implementation of a Large Static Var Compensator", *7th CEPSI*, Paper No. 3-38, Brisbane, Australia, October 1988.
16. H. Glavitsch, "Where Developments in Power System Stability Should be Directed", *Proc. Int. Symp. on Power System Stability*, Ames, Iowa, May 1985.
17. I.A. Hiskens, "Energy Functions, Transient Stability and Voltage Behaviour in Power Systems", Ph.D. Thesis, *Department of Electrical Engineering and Computer Science, University of Newcastle*, Australia, March 1990.
18. W.H. Fleming, *Functions of Several Variables*, Springer-Verlag, New York, Second Edition, 1977.
19. D.J. Hill, I.A. Hiskens and I.M.Y. Mareels, "Stability Theory of Differential/Algebraic Models of Power Systems", *11th World Congress of IFAC*, Tallin, USSR, August 1990.
20. C.N. Chong, D.J. Hill and I.A. Hiskens, "On Energy Functions for Undamped Power Systems", Technical Report EE8548, *Department of Electrical Engineering and Computer Science, University of Newcastle*, Australia, December 1985.
21. K.R. Padiyar and H.S.Y. Sastry, "Topological Energy Function Analysis of Stability of Power Systems", *International Journal of Electrical Power and Energy Systems*, Vol. 9, No. 1, January 1987.
22. T. Athay, R. Podmore and S. Virmani, "A Practical Method for the Direct Analysis of Transient Stability", *IEEE Trans. on Power Apparatus and Systems*, Vol. PAS-98, No. 2, pp 573-584, March/April 1979.
23. T.J. Overbye and C.L. DeMarco, "Voltage Security Enhancement Using Energy Based Sensitivities", Paper No. 90SM 478-8 PWRS, IEEE PES 1990 Summer Meeting, Minneapolis, July 1990.

Ian A. Hiskens (S'77 - M'80) received the B.Eng.(Elec.) degree and the B.App.Sc.(Math.) degree from the Capricornia Institute of Advanced Education, Rockhampton, Australia in 1980 and 1983 respectively. He received the Ph.D. degree from the University of Newcastle, Australia in 1990. He is currently a Planning Engineer with the Queensland Electricity Commission, Brisbane. His major research interests lie in the area of power systems analysis, in particular system dynamics and control, security, numerical techniques, and harmonics. Other research interests include nonlinear systems and control.

David J. Hill (M'76) received the B.E.(Elec.) degree and the B.Sc.(Math.) degree from the University of Queensland, Australia in 1972 and 1974 respectively. In 1976 he received the Ph.D. degree from the University of Newcastle, Australia. He is currently a Professor in Electrical Engineering and Computer Science at the University of Newcastle. His research interests are mainly in nonlinear systems and control, stability theory and power system dynamics and security. His current applied work occurs mainly in power systems.